Design and Characterization of a Microwave Feed-Forward Amplifier with Improved Wide-Band Distortion Cancellation

Y. K. Gary Hau, Vasil Postoyalko, and John R. Richardson

***Abstract*—A new approach to the design of a wide-band feed-forward amplifier (FFAMP) is presented in this paper. Phase equalizers are employed in an FFAMP to match the nonlinear delay/phase characteristics of the main and error amplifiers, improving phase balances within the cancellation loops and providing improvement in signal cancellations over a wide bandwidth. The proposed 1.7–1.9-GHz FFAMP was fabricated and characterized. The conventional FFAMP obtains an average of 15-dB third-order intermodulation (IM3) distortion cancellation over the whole bandwidth. With the phase equalizers, the proposed FFAMP achieves a further 6-dB reduction on IM3 level.**

***Index Terms*—Feed-forward amplifier, linear amplifier, linearization technique.**

I. Introduction

Feed-forward linearization has been a popular technique for reducing distortion at the output of multicarrier cellular base-station transmitters. Such technique has the advantage of superior distortion improvement over other linearization schemes [1], [2] and is suitable for dynamic channel allocation in multicarrier systems. Distortion cancellation in feed-forward amplifiers (FFAMPs) is based on the addition of two signals of the same amplitude, but 180° out of phase. The degree of cancellation is determined by the difference in amplitude and phase balances from the ideal case over the bandwidth of interest [3]. Although excellent performance has been reported on some narrow-band FFAMPs [4], [5], we have previously shown that one limiting factor on the performance of wide-band FFAMPs is due to the nonlinear dependence of phase on frequency of the main and error amplifiers, which increases phase imbalance [6].

In this paper, a design solution for reducing nonlinear phase imbalances within the cancellation loops of an FFAMP is presented. An FFAMP incorporating phase equalizers is proposed. The mechanism on compensating the nonlinear phase of the main and error amplifiers is discussed. The experimental results of the proposed 1.7–1.9-GHz FFAMP is compared with the conventional design to illustrate its feasibility.

II. FFAMP with Improved Wide-Band Cancellation

Fig. 1 shows the block diagram of the proposed FFAMP. The FFAMP consists of two loops: the signal cancellation loop and the distortion cancellation loop. A reference signal, including only the distortion generated by the main amplifier, is produced at the output of the signal cancellation loop (point C), providing the amplitude and phase differences between the input signals from each halve of the loop are zero and 180°, respectively. The reference distortion signal is amplified and recombined with the main signal at the output of the distortion cancellation loop. Perfect distortion cancellation is achieved when the amplitude and phase differences between the two distortion signals are zero and 180°, respectively, at the output. The main difference between this design over the conventional one is in the use of phase equalizers. The phase equalizers are designed to having nonlinear dependence of phase on frequency similar to that of the corresponding main and error amplifiers. As a result, the net nonlinear phase difference between the two halves of each loop is significantly reduced, minimizing the phase imbalances, especially over a wide bandwidth.

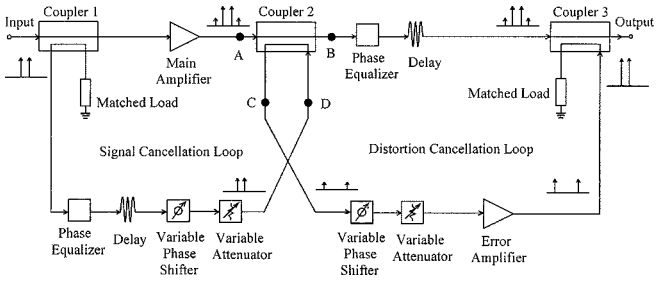

Fig. 1. Block diagram of an FFAMP with phase equalizers.

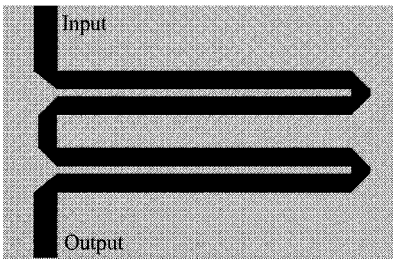

Fig. 2. Layout of the phase equalizer for main amplifier realized using two cascaded all-pass networks.

The proposed FFAMP was specified to operate from 1.7 to 1.9 GHz with an output power capability of approximately 1 W. The subcircuits shown in Fig. 1 were designed with good insertion gain/loss flatness to minimize the amplitude imbalances within the cancellation loops. The subcircuits were realized as hybrid microstrip circuits, allowing individual circuit characterization and optimization. Variable attenuators and phase shifters were included for fine tuning the performance in order to compensate any amplitude and phase imbalances introduced due to fabrication tolerance. The tuning range of the attenuator and phase shifter were 2.5 dB and 55°, respectively.

III. Phase-Equalizer Design

The phase equalizers were realized using a coupled-line all-pass network, which is also known as a C-type-section all-pass network [7], and can be easily implemented in microstrip form. Two phase equalizers were designed to approximate the nonlinear phase responses of the main and error amplifiers. The required coupling factors of the phase equalizers were first obtained following the procedures described in [7]. A coupling factor of 10 dB was initially chosen because of the ease of realizing in a microstrip coupled line. Tighter coupling is possible, but requires a more complex structure such as a Lange coupler. Due to the large nonlinear phase associated with the amplifiers, a single-stage all-pass network could not provide sufficient nonlinear phase compensation. This problem was overcome by cascading the all-pass networks, each having the same physical parameters. Fig. 2 shows the physical layout of the phase equalizer for the main amplifier with two all-pass networks. The phase equalizer for the error amplifier requires a three-stage design due to the larger nonlinear phase.

Manuscript received July 16, 1999. This work was supported by the Croucher Foundation of Hong Kong.

Y. K. G. Hau was with the School of Electronic and Electrical Engineering, The University of Leeds, Leeds LS2 9JT, U.K. and is now with the Compound Semiconductor Department, NEC Electron Devices, Shiga 5200833, Japan (e-mail: hau@ieee.org).

V. Postoyalko and J. R. Richardson are with the School of Electronic and Electrical Engineering, The University of Leeds, Leeds LS2 9JT, U.K.

Publisher Item Identifier S 0018-9480(01)00020-5.

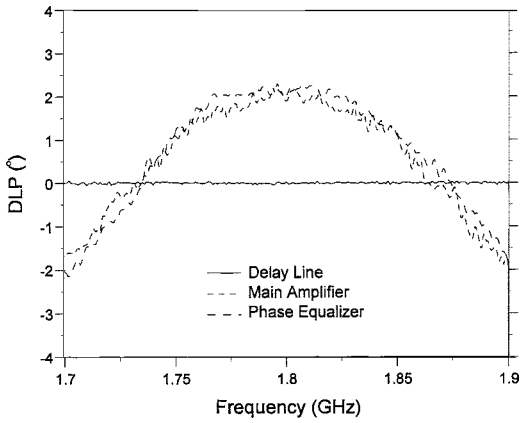

Fig. 3. Measured DLP responses of delay line, main amplifier, and phase equalizer.

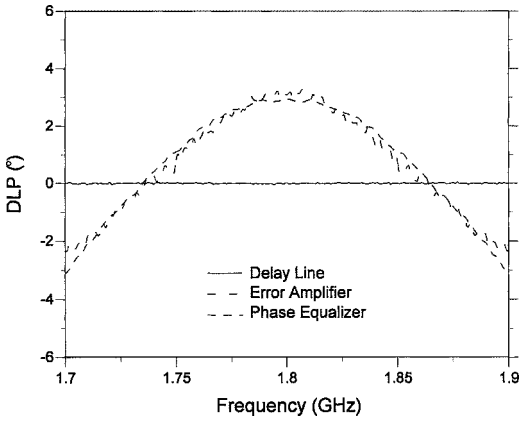

Fig. 4. Measured DLP responses of delay line, error amplifier, and phase equalizer.

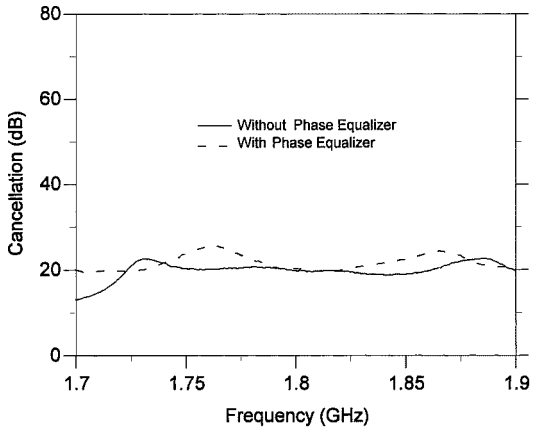

(a)

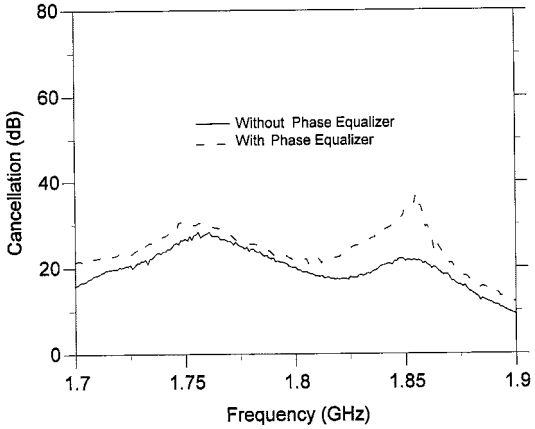

(b)

Fig. 5. Measured cancellation of the: (a) signal cancellation loop and (b) distortion cancellation loop with and without the phase equalizer.

The physical dimensions of the phase equalizers were finally optimized using HP-EEsof for the closest nonlinear phase responses to that of the corresponding amplifiers.

Fig. 3 compares the measured deviation from linear phase (DLP) responses of the phase equalizer, main amplifier, and delay line. The delay line shows a linear phase response, i.e., zero DLP, across the whole bandwidth. The nonlinear phase associated with the main amplifier varies considerably with frequency. For example, the phase difference between the delay line and main amplifier is less than $\pm 0.5^\circ$ for a 1% bandwidth with respect to the center frequency at 1.8 GHz, but increases to $\pm 2.21^\circ$ from 1.7 to 1.9 GHz. If a linear delay line is used in the signal cancellation loop, the net phase imbalance between the two halves of the loop would increase with bandwidth. Conversely, the phase equalizer shows a much closer DLP response to that of the main amplifier, allowing improvement on phase balance. Fig. 4 shows the measured DLP responses of the phase equalizer, error amplifier, and delay line. The phase equalizer also demonstrates an excellent match in DLP response to that of the error amplifier.

IV. FFAMP Measurement

A. Small-Signal Characterization

Prior to the large-signal characterization, the signal and distortion cancellation loops of the FFAMP was first individually optimized based on a linear approach [8]. The loops were measured and tuned to have the best signal cancellation over the whole frequency band by adjusting the variable attenuators and phase shifters. For the purpose of comparison, the performances of the proposed FFAMP and conventional design (without the phase equalizer) were measured.

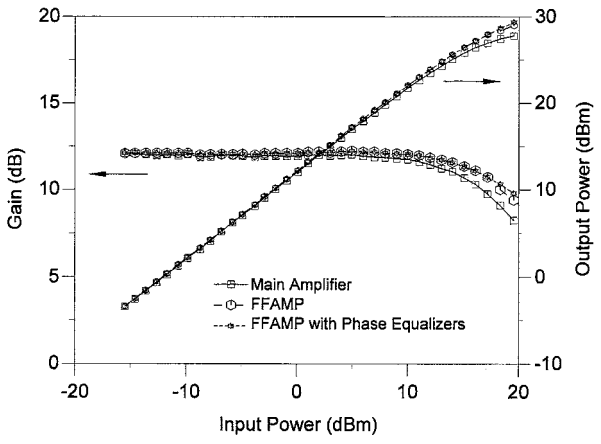

Fig. 6. Measured gain and output power of the amplifiers for a single-tone input at 1.8 GHz.

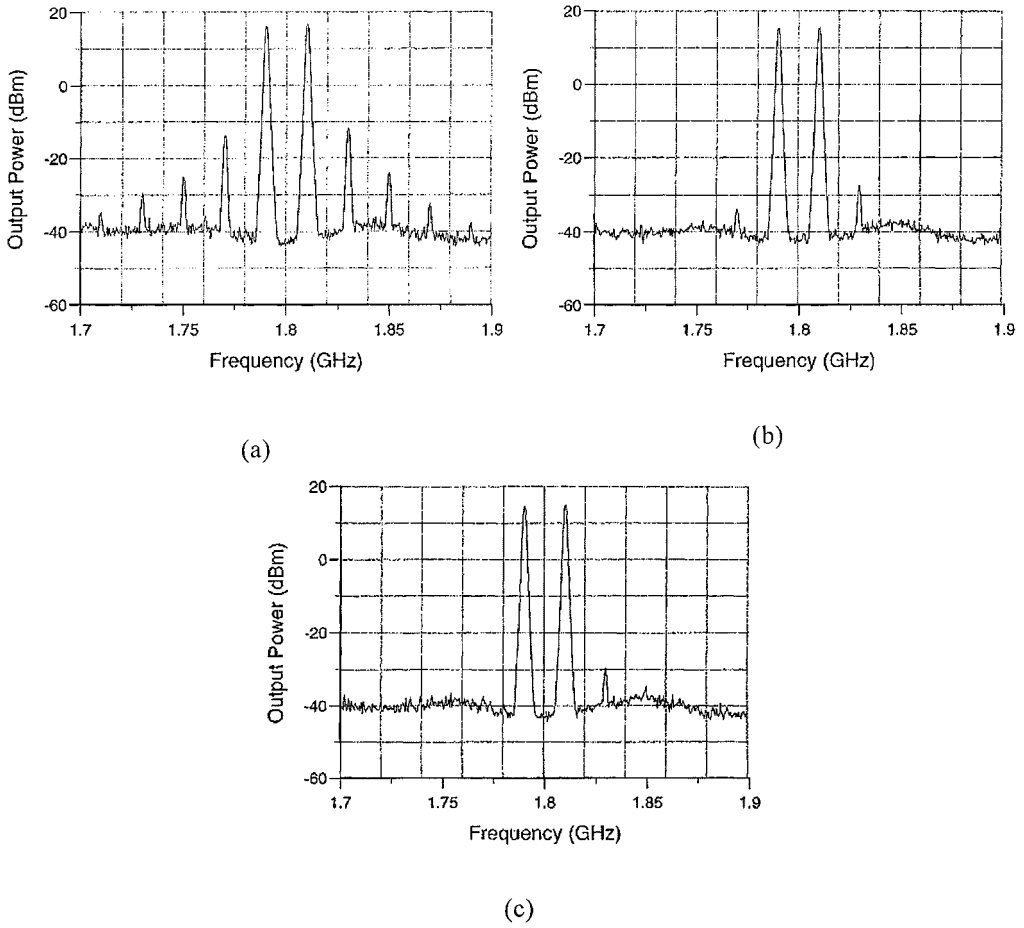

Fig. 7. Measured output power spectrum of the: (a) main amplifier, (b) conventional FFAMP, and (c) FFAMP with phase equalizers for a two-tone input at 1.79 and 1.81 GHz.

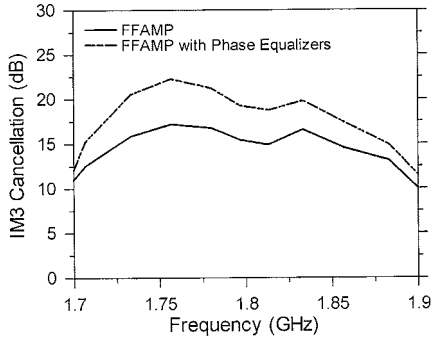

Fig. 8. Measured IM3 cancellation of the conventional FFAMP and FFAMP with phase equalizers from 1.7 to 1.9 GHz.

For the optimization of the signal cancellation loops of the FFAMPs, point B in Fig. 1 was disconnected and replaced by a 50-Ω termination. The cancellation response was measured between input and point C on the HP8510 vector network analyzer. The input signal to this loop represents the main signal to be canceled at the output of the loop. The measured cancellations are shown in Fig. 5(a). The cancellation is improved over the whole frequency band after the use of the phase equalizer. The average improvement of cancellation is over 3 dB across the bandwidth compared to the conventional design.

The measurement and optimization procedures for the distortion cancellation loops were similar to that of the signal cancellation loops. Referring to Fig. 1, the cancellation response was measured between point A and output, whereas point D was disconnected and replaced by a 50-Ω termination. The input signal represents the intermodulation product generated by the main amplifier required for cancellation at the output. Fig. 5(b) shows the measured cancellations, demonstrating an average cancellation improvement of better than 4 dB with the use of the phase equalizer. The improvement in the distortion cancellation loop is higher than that of the signal cancellation loop due to a higher degree of nonlinear phase response being compensated by the phase equalizer for the error amplifier than the main amplifier (refer to Figs. 3 and 4).

B. Large-Signal Characterization

The proposed and conventional FFAMPs were constructed from the optimized cancellation loops. The FFAMPs were first subjected to a single-tone input test at 1.8 GHz. Fig. 6 shows the measured gain and output power as a function of input power. The output power measured at a 1-dB compression point is improved by 3.2 dB for both of the feed-forward cases. No significant difference in characteristic is observed between the two FFAMPs, suggesting no degradation in performance with the introduction of phase equalizers.

The distortion characteristics of the FFAMPs were examined by a standard two-tone test. The amplifiers, with and without feed-forward linearization, were tested over a range of input frequencies to verify the cancellation of distortions across the whole frequency band. Fig. 7 shows the measured output frequency spectrum of the amplifiers for a

two-tone input at 1.79 and 1.81 GHz. The conventional FFAMP provides a 16-dB cancellation on the third-order intermodulation (IM3) distortions compared to the main amplifier without linearization. A similar degree of cancellation is observed for other in-band distortion products. When the phase equalizers were used, a further improvement of 4 dB on IM3 cancellation is achieved. Fig. 8 shows the IM3 cancellation over the frequency band of interest obtained from several two-tone measurements. The proposed FFAMP attains better characteristic over the whole bandwidth with a maximum of 6-dB cancellation improvement compared to the conventional design.

V. Conclusions

A new topology of FFAMP with improved wide-band performance has been presented in this paper. Phase equalizers were designed to approximate the nonlinear dependence of phase on frequency of the main and error amplifiers, reducing the nonlinear phase imbalances within the cancellation loops. A 1.7–1.9-GHz FFAMP incorporating the phase equalizers was designed, fabricated, and tested. The proposed FFAMP achieved an improved cancellation characteristic over the whole bandwidth, with a maximum of 6-dB IM3 distortion improvement, compared to the conventional design. This demonstrates the wide-band distortion characteristic of FFAMPs can be improved with the use of phase equalizers.

References

[1] J. K. Cavers, "Adaptive behavior of a feedforward amplifier linearizer," *IEEE Trans. Veh. Thechnol.*, vol. 44, pp. 31–39, Feb. 1995.

[2] S. Narahashi and T. Nojima, "Extremely low-distortion multi-carrier amplifier—Self-adjusting feedforward amplifier," in *Proc. IEEE Int. Commun. Conf.*, June 1991, pp. 1485–1490.

[3] Y. K. G. Hau, V. Postoyalko, and J. R. Richardson, "Sensitivity of distortion cancellation in feedforward amplifiers to loops imbalances," in *IEEE MTT-S Int. Microwave Symp. Dig.*, Denver, CO, June 1997, pp. 1695–1698.

[4] J. P. Dixon, "A solid-state amplifier with feedforward correction for linear single-sideband applications," in *Proc. IEEE Int. Commun. Conf.*, 1986, pp. 728–732.

[5] PST Inc., "High power feed forward amplification systems," *Microwave J.*, vol. 37, no. 2, pp. 128–133, Feb. 1994.

[6] Y. K. G. Hau, V. Postoyalko, and J. R. Richardson, "Compensation of amplifier nonlinear phase response to improve wideband distortion cancellation of feedforward amplifiers," *Electron. Lett.*, vol. 33, no. 6, pp. 500–502, Mar. 1997.

[7] S. O. Scanlan and J. D. Rhodes, "Microwave allpass networks—Part I," *IEEE Trans. Microwave Theory Tech.*, vol. 16, pp. 62–71, Feb. 1968.

[8] K. Konstantinou, P. Gardner, and D. K. Paul, "Optimization method for feedforward linearization of power amplifiers," *Electron. Lett.*, vol. 29, no. 29, pp. 1633–1635, Sept. 1993.

Design of a Low-Supply-Voltage High-Efficiency Class-E Voltage-Controlled MMIC Oscillator at C-Band

Frank Ellinger, Urs Lott, and Werner Bächtold

***Abstract*—In this paper, a monolithically integrated voltage-controlled class-E tuned oscillator for C-band has been designed and measured. Large-signal optimization was performed using analytically calculated starting values to reach high efficiencies at ultra-low supply voltages down to 0.9 V. The range of the tuning voltage is from 0 to the supply voltage. With a supply voltage of 1.8 V, an output power of 6.5 dBm, an efficiency of 43%, and a tuning range of 150 MHz is achieved at a center frequency of 4.4 GHz. With a supply voltage of only 0.9 V, the efficiency is 36%, with an output power of 1.1 dBm, and a tuning range of 80 MHz at a frequency of 3.6 GHz. Chip size is less than 1 mm^2.**

***Index Terms*—MESFETs, MMICs, oscillators.**

I. Introduction

For portable communications equipment, the power consumption has to be minimized. In receivers especially, there is the trend to ever lower supply voltages. The RF section of these receivers consists mainly of low-noise amplifiers (LNAs), mixers, and oscillators. LNAs operating at C-band have been previously reported using supply voltages below 1.5 V [1]. A variety of passive mixers that require no dc supplies have been reported. However, there are few references available on oscillators using low supply voltages. Generally, the efficiency (RF/dc power) of oscillators reduces with decreased supply voltages, thus, most designs require relatively high supply voltages [2]–[4]. Table I shows a summary of oscillators at microwave frequencies with state-of-the-art efficiencies. The lowest supply voltage was 2.0 V, as reported in [5]. An efficiency (η) of 61% at L-band has been reached with a 0.25-μm high electron-mobility transistor (HEMT) process. However, note that except for [3], none of the listed high-efficiency oscillators has frequency tuning.

The purpose of this paper was the design of a highly efficient class-E C-band voltage-controlled oscillator (VCO) with ultra-low supply voltages from 1.8 to 0.9 V, which required minimum chip size.

Large-signal optimization was performed using starting values that were analytically calculated by using simple equivalent circuits. A standard 0.6-μm E/D MESFET GaAs foundry process (Triquint TQTRx, Hillsboro, OR) was used for the design.

II. Approximate Analysis

The major parts of the circuit are the class-E output, the feedback in the source, and the resonator.

A. Class-E Output and Bias

Fig. 1 shows the equivalent class-E output network of the VCO. $R_{\rm eff}$ is the effective load resistance, which is the sum of the load resistance and the resistive parasitics. $V_{\rm eff}$ is the effective dc voltage, which is determined by the saturation voltage, the source voltage drop of the bias network, and the resistive losses of the FET. $L_{\rm eff}$ is the class-E inductance L_x, including the output bondwire $L_{\rm bond}$ ($L_{\rm eff} = L_x + L_{\rm bond}$).

Manuscript received July 26,1999.

The authors are with the Laboratory for Electromagnetic Fields and Microwave Electronics, Swiss Federal Institute of Technology Zurich, CH-8092 Zürich, Switzerland (e-mail: ellinger@ifh.ee.ethz.ch).

Publisher Item Identifier S 0018-9480(01)00018-7.